Metamagnetism in $CePd_5Ge_3$

2013 J. Phys.: Condens. Matter 25 126001

(http://iopscience.iop.org/0953-8984/25/12/126001)

IOP PUBLISHING JOURNAL OF PHYSICS: CONDENSED MATTER
J. Phys.: Condens. Matter **25** (2013) 126001 (6pp) doi:10.1088/0953-8984/25/12/126001

Metamagnetism in $CePd_5Ge_3$

Daniel Gnida[1], Piotr Wiśniewski[1], Alexander V Gribanov[2], Yurii D Seropegin[2] and Dariusz Kaczorowski[1]

[1] Institute of Low Temperature and Structure Research, Polish Academy of Sciences, 50-950 Wrocław, Poland
[2] Chemistry Department, M V Lomonosov Moscow State University, 119899 Moscow, Russia

E-mail: d.gnida@int.pan.wroc.pl

Received 14 November 2012
Published 28 February 2013
Online at stacks.iop.org/JPhysCM/25/126001

Abstract
Metamagnetic transitions in $CePd_5Ge_3$ were investigated by means of low-temperature magnetization, magnetic susceptibility, electrical resistivity and magnetoresistivity measurements. In transverse magnetic fields applied in a direction close to the *b*-axis the antiferromagnetic structure of the compound undergoes two successive transitions, first to a spin-flop phase and then to a paramagnetic phase with field-induced ferromagnetic-like alignment of the Ce magnetic moments. In contrast, a single anomaly occurs in the magnetic field dependences of the resistivity in a transverse magnetic field applied close to the *c*-axis, which reflects a direct transition from antiferromagnetic to paramagnetic state. Such behavior is in agreement with theoretical descriptions of metamagnetic transitions in uniaxial antiferromagnets. The experimental magnetic and electrical transport data indicate that the *b*-axis is the easy axis of magnetization in $CePd_5Ge_3$.

1. Introduction

Cerium-based intermetallics are continuously attracting much attention due to the large diversity of their correlated-electron behavior resulting from variable hybridization between their 4f-electronic states and electrons from the s, p and/or d bands of neighboring atoms. Particular interest has been focused on ternary silicides and germanides containing d-electron noble metals, because of the rich spectrum of anomalous properties ranging from complex long-range magnetic order to heavy-fermion ground states to intermediate-valence behavior.

The germanide $CePd_5Ge_3$ crystallizes with the orthorhombic YNi_5Si_3-type crystal structure (space group *Pnma*, $Z = 4$) [1]. Neutron diffraction, magnetic susceptibility and heat capacity measurements have revealed that the compound orders antiferromagnetically below $T_N = 1.9$ K [2, 3]. The cerium magnetic moments have been found to form a simple commensurate antiferromagnetic structure with a propagation vector $\mathbf{k} = (001)$ [3]. However, the direction of these moments has not been established yet. The magnetic susceptibility data have indicated well localized magnetic moments of stable Ce^{3+} ions, while the small value of the electronic specific heat coefficient ($\gamma = 21$ mJ mol^{-1} K^{-2}), the tiny reduction in the magnetic entropy at T_N ($S_m = 0.9\,R\ln 2$) and the absence of Kondo features in the electrical resistivity have shown that the electronic correlations in $CePd_5Ge_3$ are rather weak [2, 4]. In the ordered region, both the isothermal magnetization and the longitudinal magnetoresistance have shown behavior characteristic of spin reorientation (with the critical field $B_c = 1.2$ T at $T = 1.8$ K); however, the nature of this transition has not been clarified yet [2]. Metamagnetic transitions are common in antiferromagnets and, depending on the number of magnetic sublattices, strength of the magnetocrystalline anisotropy, and/or temperature, the spins may be reoriented to intermediate ferrimagnetic or spin-flop phases or directly to a paramagnetic phase with field-forced parallel alignment of moments [5].

In order to determine the character of the metamagnetic transition in $CePd_5Ge_3$, we performed low-temperature measurements of magnetization, magnetic susceptibility, electrical resistivity and magnetoresistivity in applied magnetic fields up to 9 T.

2. Experimental details

A sample of $CePd_5Ge_3$ was prepared by arc-melting stoichiometric amounts of elements in a Ti-gettered argon

atmosphere. The button was flipped over and remelted several times to ensure good homogeneity. The final losses were less than 1 wt%. The alloy was then sealed in an evacuated quartz tube and annealed at 600 °C for four days. After the heat treatment the ampule was quenched in cold water.

Since anisotropy of the magnetic properties of polycrystalline samples of $CePd_5Ge_3$ has previously been reported [2], we examined an irregularly shaped sample obtained by cutting off outer parts of the button on a four-circle x-ray diffractometer equipped with a CCD camera. The obtained images showed well defined reflections, characteristic of single-crystalline material. This indicated that the sample was polycrystalline but coarsely grained, actually consisting of several large single-crystalline grains (of about 1 mm diameter) and some uncountable fine crystallites. Moreover, the large grains all had similar (within a range of several degrees) orientation of their crystallographic axes. Then, from that sample we cut a rectangular parallelepiped, with the longest edge along the *a*-axes and two shorter edges along the *b*- and *c*-axes of these large grains. A sample prepared in such a way might be regarded as a strongly 3D-textured polycrystalline one, or as an approximation of poor quality (because of strong mosaicity) single crystal. This was the sample on which we carried out magnetic and magnetotransport measurements. In consequence, when describing results obtained in an applied magnetic field, B, we denote its directions as $B \parallel c$ and $B \parallel b$, and the electrical current direction as parallel to the *a*-axis, keeping in mind that this is a rather rough approximation. These orientations of the magnetic field with respect to the sample and the current are schematically presented in figures 4(a) and 5(a).

The magnetic measurements were performed in the temperature range of 0.48–300 K and in applied magnetic fields up to 7 T using a Quantum Design MPMS-XL SQUID magnetometer equipped with an iHelium3 sub-Kelvin cooling system. The temperature and magnetic field variations of the electrical resistivity were measured in the temperature interval of 0.35–300 K and at magnetic fields up to 9 T using a Quantum Design PPMS platform.

3. Results and discussion

3.1. Magnetic properties

Earlier studies of the magnetic susceptibility of $CePd_5Ge_3$ have shown that above 100 K it follows a Curie–Weiss law with an effective magnetic moment of $\mu_{\mathrm{eff}} = 2.6\ \mu_{\mathrm{B}}$ and a paramagnetic Curie temperature of $\theta = -35$ K [2, 4]. The experimental value of μ_{eff} was close to the calculated one for a free Ce^{3+} ion, $\mu_{\mathrm{eff}} = 2.54\ \mu_{\mathrm{B}}$, thus indicating the presence of well localized magnetic moments carried by stable Ce^{3+} ions. In turn, the negative sign of θ pointed to antiferromagnetic exchange interactions, and signaled the antiferromagnetic phase transition, observed in the heat capacity and electrical resistivity data [2, 4], and corroborated in the neutron diffraction experiment [3]. However, any clear evidence for magnetic ordering in the bulk magnetic data of the compound has been lacking so far.

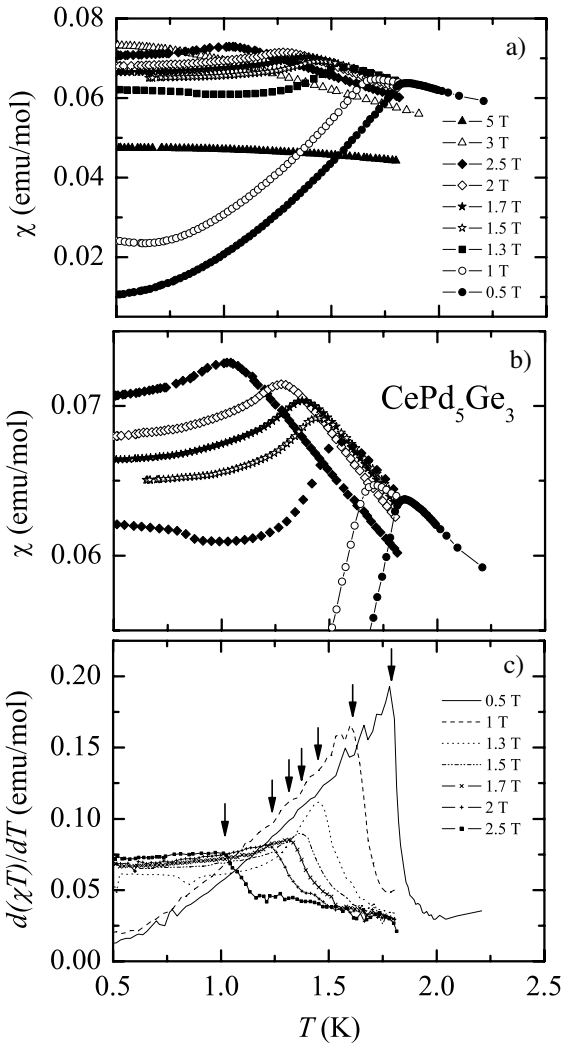

Figure 1. (a) The low-temperature dependence of the molar magnetic susceptibility of $CePd_5Ge_3$ measured in various magnetic fields applied along the *b*-axis. (b) Zoomed view of selected data from (a). (c) The temperature variation of the derivative $\mathrm{d}(\chi T)/\mathrm{d}T$. The arrows mark the antiferromagnetic phase transition.

Figures 1(a) and (b) show the temperature variations of the magnetic susceptibility of $CePd_5Ge_3$, measured below 2 K in different magnetic fields applied along the *b*-axis (the magnetic measurements performed at higher temperatures just confirmed previous findings, and hence the results are not shown). A pronounced maximum in $\chi(T)$ taken in a field of 0.5 T manifests the antiferromagnetic phase transition at $T_{\mathrm{N}} = 1.85$ K. With increasing magnetic field up to 2.5 T, this anomaly gradually shifts to lower temperatures, in a manner typical for antiferromagnetic systems (figure 1(c)). Simultaneously, the magnitude of the magnetic susceptibility at the maximum increases. However, in fields of $B = 1$ and 1.3 T, $\chi(T)$ shows a shallow minimum in the ordered region and levels off with T going to zero, instead of the monotonic decrease expected for simple antiferromagnets. In stronger fields, the susceptibility saturates at high values, only slightly smaller than those attained at the maximum. Finally, for $B \geq 3$ T, the low-temperature magnetic response of $CePd_5Ge_3$ is entirely different from that characteristic of antiferromagnets, namely no maximum in $\chi(T)$ is seen;

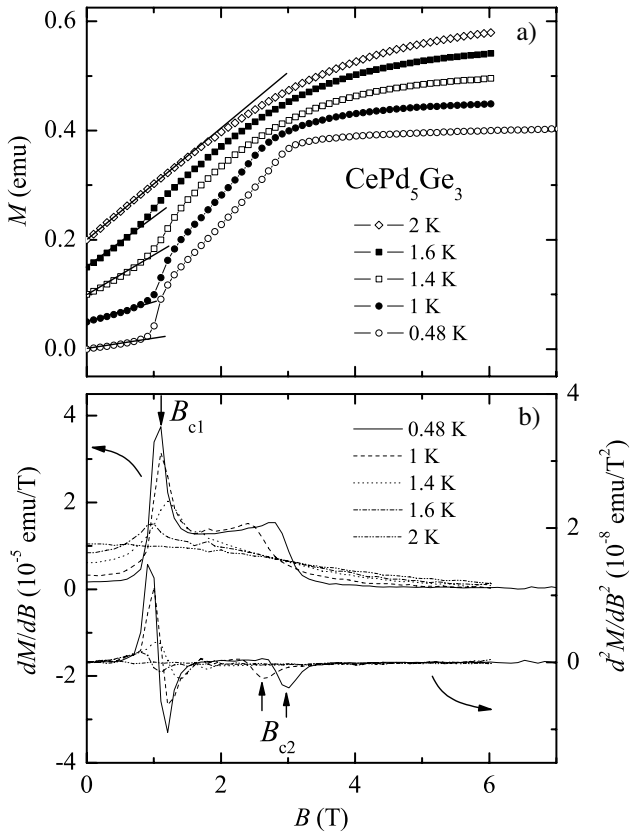

Figure 2. (a) Magnetic field variations of the magnetization in $CePd_5Ge_3$ measured at several different temperatures, in field applied along the *b*-axis. For clarity, the isotherms are shifted upwards by multiplies of 0.05 emu. The solid lines emphasize linear variations in weak fields. (b) Magnetic field derivatives of the magnetization data from (a). The arrows mark the metamagnetic phase transitions.

instead, the susceptibility saturates at low temperatures, and its magnitude becomes roughly inversely proportional to the strength of the magnetic field. Such evolution of $\chi(T)$ in external magnetic fields signals significant changes in the magnetic structure of the compound, apparently of metamagnetic nature.

More evidence for the metamagnetism in $CePd_5Ge_3$ comes from the behavior of the isothermal magnetization measured in the ordered state as a function of the magnetic field strength. As shown in figure 2(a), initially the magnetization increases linearly with rising field, with the slope in $M(B)$ decreasing with decreasing temperature, just as expected for antiferromagnets. However, in a field B_{c1} of about 1 T, the $M(B)$ curves exhibit clear kinks, which are more pronounced the lower the temperature is. This is more clearly seen as sharp peaks in the first derivative of the magnetization with respect to the magnetic field, $dM(B)/dB$, displayed in figure 2(b). Further increase of the magnetic field strength results in an increase of the magnetization with some moderate bending in $M(B)$, observable up to a field B_{c2}, at which another distinct change in the slope of $M(B)$ occurs. The value of B_{c2} depends strongly on the temperature (see also figure 2(b)). For example, at $T = 0.48$ K, the upper transition takes place at $B_{c2} = 3$ T, while at $T = 1.2$ K, it shifts

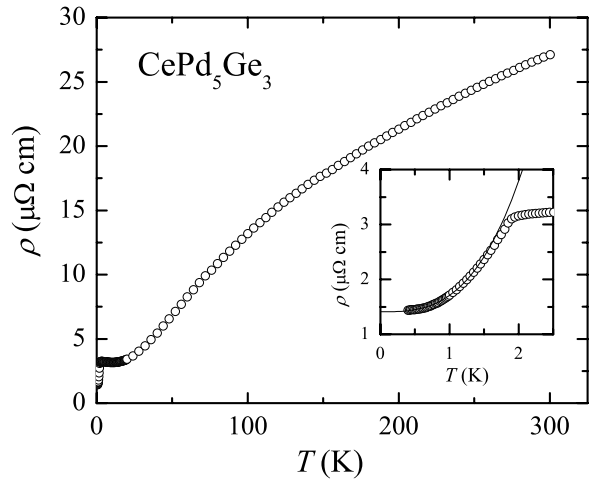

Figure 3. The temperature dependence of the electrical resistivity of $CePd_5Ge_3$. Inset: low-temperature window of $\rho(T)$. The solid line represents the power law behavior of $\rho(T)$ at low temperatures.

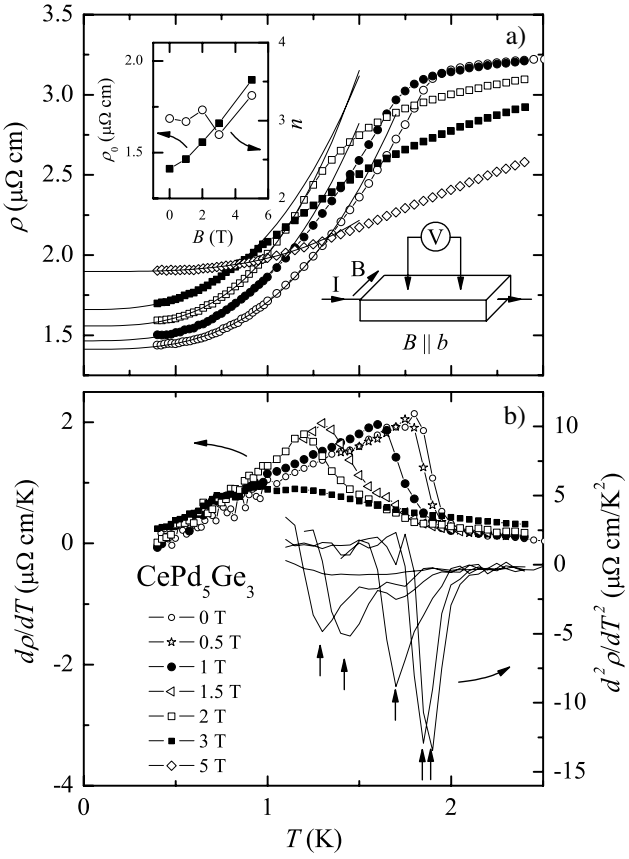

Figure 4. (a) The low-temperature dependence of the electrical resistivity of $CePd_5Ge_3$ in zero and applied transverse magnetic field $B \parallel b$. Inset: $\rho_0(B)$ and power factor n as a function of magnetic field (see the details in the text). (b) First and second derivative of $\rho(T)$. The arrows mark the transition temperatures.

down to $B_{c2} \simeq 2.1$ T. This behavior is likely due to another metamagnetic phase transition.

3.2. Electrical transport

The electrical resistivity of $CePd_5Ge_3$ is shown in figure 3. The overall behavior of $\rho(T)$ is similar to that reported

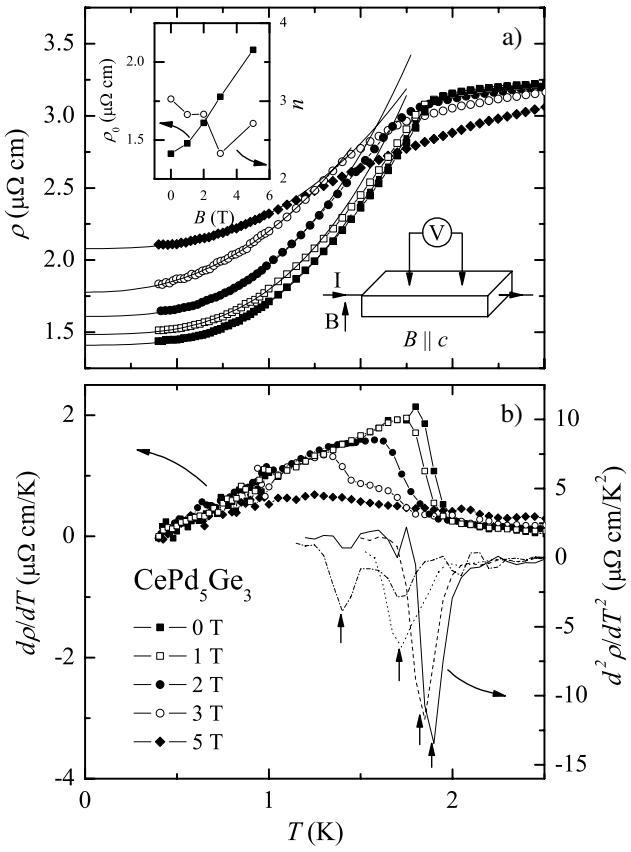

Figure 5. The same as figure 4 but for applied transverse magnetic field $B \parallel c$.

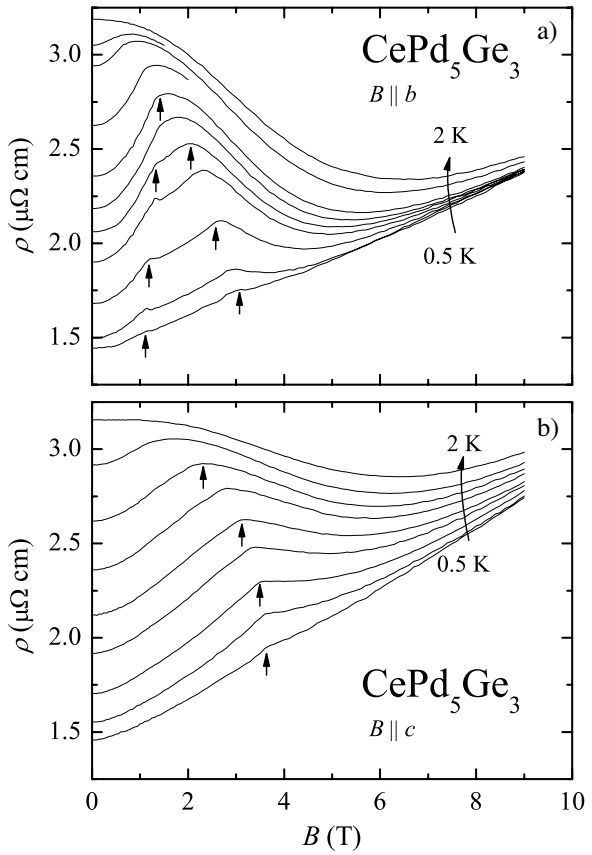

Figure 6. (a), (b) The magnetic field dependences of the electrical resistivity of $CePd_5Ge_3$ for two different orientations of the magnetic field, $B \parallel b$ and $B \parallel c$, respectively. The arrows mark the transitions to different spin states according to the schematically presented figures in the phase diagram in figure 7.

previously [2, 4]. It is worth noting that the residual resistivity, $\rho_0 = 1.41$ $\mu\Omega$ cm, is very small, which together with large value of the ratio $\rho_{300\,\mathrm{K}}/\rho_0 = 19.2$ points to good quality of the investigated sample. The antiferromagnetic ordering manifests itself as a sudden drop in the resistivity below T_N. The low temperature antiferromagnetic region of $\rho(T)$ can be described by a power law relation $\rho(T) = \rho_0 + aT^n$ with $n \simeq 3$ and $a = 0.3$ $\mu\Omega$ cm K^{-3}.

The inset of figure 4(a) shows that the magnetic field applied along the b-axis hardly affects the power factor n but causes a monotonic increase of the value ρ_0. The small drop of n observed at 3 T might be due to the transition to the paramagnetic state. The first and second derivatives of $\rho(T)$ with respect to the magnetic field presented in figure 4(b) show that increasing the strength of the field results in shifting the phase transition to lower temperatures with gradual smearing of the anomaly and its subsequent suppression for $B \geq 3$ T.

Figure 5(a) depicts the temperature dependence of the electrical resistivity of $CePd_5Ge_3$ in the transverse magnetic field $B \parallel c$. At first glance the curves $\rho(T, B \parallel b)$ and $\rho(T, B \parallel c)$ are very similar. Fitting $\rho(T, B \parallel c)$ with the power law function yields power factors n of comparable values and with anomalous behavior at $B = 3$ T but exhibiting a tendency to decrease with magnetic field strength. The ρ_0 term also increases monotonically with magnetic field strength but faster than for $B \parallel b$. For instance, at 5 T, ρ_0 is equal to 1.9 $\mu\Omega$ cm and 2.08 $\mu\Omega$ cm for $B \parallel b$ and $B \parallel c$, respectively. Moreover, the derivatives of $\rho(T, B)$ presented in figure 5(b) indicate that the transition to the paramagnetic state is suppressed by the magnetic field somewhat higher when $B \parallel c$ than when $B \parallel b$. In order to clarify this discrepancy we carried out measurements of the electrical resistivity as a function of magnetic field.

The magnetic field dependence of the electrical resistivity was measured for $CePd_5Ge_3$ at several temperatures in the range of 0.5–2 K. As shown in figure 6(a), for $B \parallel b$ at low temperatures there are two anomalies in $\rho(B)$. The first anomaly is weakly temperature dependent while the second one gradually shifts to lower magnetic fields with increasing temperature. This behavior agrees with that observed in the magnetization data (with anomalies B_{c1} and B_{c2}, respectively, see figure 2). At $B \geq 1.4$ K these two anomalies merge into a single one—a maximum in $\rho(B)$. This maximum shifts to lower magnetic fields with rising temperature and finally vanishes above T_N.

It is evident from figure 6(a) that at 2 K, in the paramagnetic state, the magnetoresistivity is negative. However, at about $B = 6.5$ T a shallow minimum is observed pointing to an additional positive contribution to the magnetoresistivity. The positive contribution to the magnetoresistivity increases with decreasing temperature. In the antiferromagnetic state (fields up to B_{c1} and/or B_{c2}),

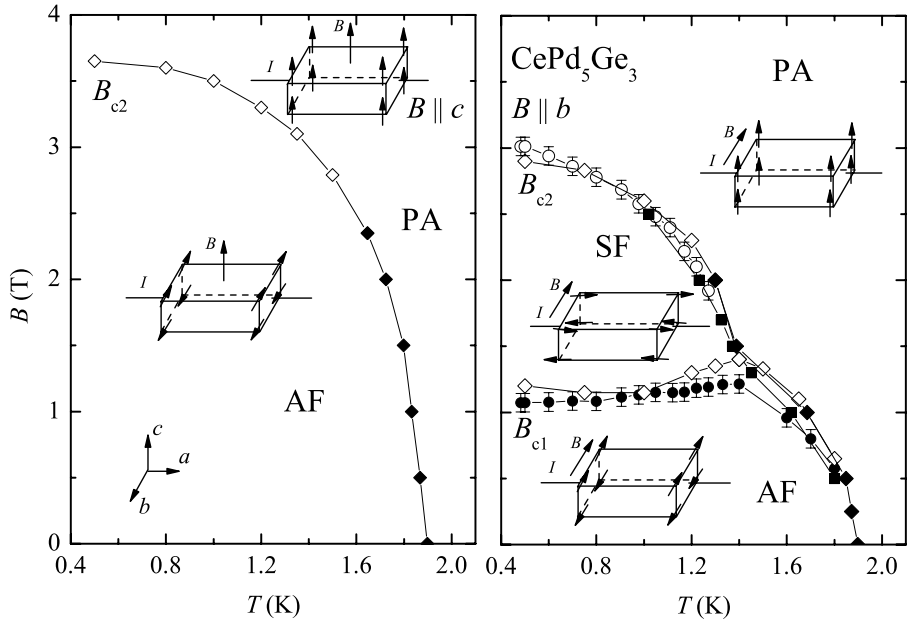

Figure 7. The magnetic phase diagram of $CePd_5Ge_3$ for two different orientations of the transverse magnetic field, $B \parallel c$ (left) and $B \parallel b$ (right). The filled circles correspond to the maxima in $dM/dB(B)$, the open circles denote the minima in $d^2M/dB^2(B)$, the squares refer to the maxima in $d(\chi T)/dT(T)$ and the open and filled diamonds refer to $d^2\rho/dB^2(B)$ and $d^2\rho/dT^2(T)$, respectively. The different sublattice magnetization states (denoted as AF—antiferromagnet, SF—spin-flop phase and PM—paramagnet) are presented schematically in the appropriate regions.

the magnetoresistivity is positive. Above B_{c2}, $\rho(B)$ initially decreases but further strengthening of the magnetic field results in a minimum, in similar manner to that for $\rho(B)$ measured at 2 K. This minimum shifts to lower magnetic fields and, finally, at the lowest temperature, totally vanishes. It is especially worth noting that at high magnetic field and low temperature the $\rho(B)$ variation is linear.

In contrast to the $B \parallel b$ results, the measurements performed in the $B \parallel c$ configuration revealed a single anomaly in $\rho(B)$ at all temperatures (figure 6(b)). Generally, $\rho(B)$ behaves with changing temperature in a similar manner to that for $B \parallel b$, and in the paramagnetic state the $\rho(B, 2\ \mathrm{K})$ curve resembles that obtained for the $B \parallel b$ configuration, with a minimum at the same magnetic field of $B = 6.5$ T. On the other hand, a difference in the absolute value of the magnetoresistivity points to anisotropic behavior of our polycrystalline sample with respect to the direction of the applied magnetic field. The magnetoresistivity, $MR = (\rho(B) - \rho(B = 0))/\rho(B = 0)$, attains at 9 T -23% and -5.4% for $B \parallel b$ and $B \parallel c$, respectively. With reducing temperature the minimum shifts to lower magnetic fields and vanishes below 1 K, indicating that the positive contribution to the magnetoresistivity dominates in the whole magnetic field range. Anisotropy of the magnetoresistivity is also evident at the lowest temperature of 0.5 K, where $\rho(B)$ also changes linearly with increasing magnetic field, and $MR = -88\%$, which is much larger than the -65% observed for $B \parallel b$.

The overall magnetic field behavior of the magnetoresistivity might be explained as a result of two contributions: one due to electron-spin scattering resulting from s–d interaction in localized antiferromagnetic metals [6, 7], and another due to the magnetic field effect on conduction electrons. In the theoretical model of Yamada and Takada [6, 7], conduction electrons are scattered by fluctuations of localized magnetic moments, with which they interact through weak s–d interaction. According to [6, 7], up to B_{c1}, the magnetoresistivity due to s–d interaction in the antiferromagnetic state is positive. In the paramagnetic state (above B_{c1} or B_{c2}), the magnetic field strengthens the effective field acting on the localized spins and suppresses their fluctuations, thus leading to a negative contribution to the magnetoresistivity. Apart from the magnetic contribution to the magnetoresistivity one must also take into account the cyclotron motion of the conduction electrons in the magnetic field, which depends on the factor $(\omega_c\tau)^2$, where ω_c is the cyclotron frequency and τ is the life time of the conduction electrons. It seems that this contribution is responsible for the minima of $\rho(B)$ that appear in the paramagnetic state of $CePd_5Ge_3$ above B_{c1} or B_{c2}. Moreover, at low temperatures, $\rho(B) \propto B$ in high magnetic fields. This linear behavior of the magnetoresistivity probably originates from suppression of magnetic s–d interaction with increasing ratio of B/T. This presumption is based on the Yamada and Takada results, which indicate that within the first Born approximation the resistivity due to electron-spin scattering in the paramagnetic low-temperature region (for $B > B_{c1}$ or $B > B_{c2}$) decreases with increasing B and becomes zero for $B \to \infty$ [7].

4. Conclusions

The magnetization and magnetotransport data of $CePd_5Ge_3$ presented here clearly reveal the metamagnetic transitions from the antiferromagnetic state to the paramagnetic state. Determination of the characteristic magnetic fields B_{c1} and B_{c2} allowed us to construct the magnetic phase diagrams presented in figure 7. For $B \parallel c$, with increasing temperature

B_{c2} monotonically decreases down to $T = T_N$. The single phase separation line corresponds to the metamagnetic transition in which the antiferromagnetic ordering directly transforms into the magnetic field-forced paramagnetic state. In contrast, for $B \parallel b$ an intermediate phase of ferrimagnetic or spin-flop character is observed between B_{c1} and B_{c2}. With increasing temperature, B_{c1} hardly changes, whereas B_{c2} distinctly decreases. The two characteristic fields merge near $T \simeq 1.4$ K into a single critical field, which with further increase in temperature smoothly decreases and attains zero at $T = T_N$. As can be inferred from figure 2, the change in $M(B)$ that occurs at B_{c1} is very sharp and the derivative $dM(B)/dB$ has a character reminiscent of first-order transitions. In turn, the magnetization anomalies at B_{c2} are less pronounced. One might expect that in the intermediate phase of $CePd_5Ge_3$ the cerium magnetic moments would undergo a gradual rotation towards the direction of the external magnetic field and the onset of the paramagnetic state above B_{c2} would be of continuous phase transition type.

Based on the derived magnetic phase diagrams for $B \parallel b$ and $B \parallel c$ one can presume that the easy magnetization direction in $CePd_5Ge_3$ is parallel to the crystallographic b-axis. This conclusion is due to the fact that in antiferromagnetic systems a spin-flop phase is typically observed for magnetic fields applied along the magnetic moments, here for $B \parallel b$. When a magnetic field is applied perpendicular to the moments, usually only the second-order phase transition occurs, as found in $CePd_5Ge_3$ for $B \parallel c$. Obviously, the inferred directions of the magnetic moments in the compound studied should be verified in a study of high quality single crystals. A neutron diffraction experiment in an applied magnetic field would also be highly appropriate for validation of the actual nature of the magnetic phases of $CePd_5Ge_3$, revealed in the present work from the bulk magnetic and electrical transport data.

References

[1] Seropegin Yu D, Gribanov A V, Chernyshov V V, Rybakov V B and Bodak O I 1998 *J. Alloys Compounds* **274** 182
[2] Hossain Z, Takabatake T, Geibel C, Gegenwart P, Oguro I and Steglich F 2001 *J. Phys.: Condens. Matter* **13** 4535
[3] Stockert O, Hossain Z, Deppe M, Hohlwein D and Geibel C 2004 *J. Magn. Magn. Mater.* **272** e479
[4] Kaczorowski D, Czopnik D, Suski W, Nikiforov V N and Gribanov A V 2001 *Solid State Commun.* **117** 373
[5] Stryjewski E and Giordano N 1977 *Adv. Phys.* **26** 487
[6] Yamada H and Takada S 1973 *J. Phys. Soc. Japan* **34** 51
[7] Yamada H and Takada S 1973 *Prog. Theor. Phys.* **49** 1401